

Spin Waves in Ultrathin Ferromagnets: Intermediate Wave Vectors

A. T. Costa

Depto. de Ciências Exatas, Universidade Federal de Lavras,
37200-000 Lavras, Minas Gerais, Brazil

R. B. Muniz

Instituto de Física, Universidade Federal Fluminense,
24210-340 Niterói, Rio de Janeiro, Brazil

D. L. Mills

Department of Physics and Astronomy,
University of California, Irvine, California 92697 U.S.A.

Abstract

Our earlier papers explore the nature of large wave vector spin waves in ultrathin ferromagnets, and also the properties and damping of spin waves of zero wave vector, at the center of the two dimensional Brillouin zone, with application to FMR studies. The present paper explores the behavior of spin waves in such In_s at intermediate wave vectors, which connect the two regions. For the case of Fe_s on $\text{Au}(100)$, we study the wave vector dependence of the linewidth of the lowest frequency mode, to find that it contains a term which varies as the fourth power of the wave vector. It is argued that this behavior is expected quite generally. We also explore the nature of the eigenvectors of the two lowest lying modes of the In_s , as a function of wave vector. Interestingly, as wave vector increases, the lowest mode localizes onto the interface between the In_s and the substrate, while the second mode evolves into a surface spin wave, localized on the outer layer. We infer similar behavior for a Co_s on $\text{Cu}(100)$, though this evolution occurs at rather larger wave vectors where, as we have shown previously, the modes are heavily damped with the consequence that identification of distinct eigenmodes is problematical.

I. INTRODUCTION

The nature of spin motions in ultrathin ferromagnetic films and more generally in magnetic nanostructures is a fundamental topic, important also from the point of view of applications. It is the motion of magnetic moments within ultrathin films that allow giant magnetoresistive read heads respond to the bits on hard discs, and more recently in the elements incorporated into prototype magnetic random access memory (MRAM). Thus, issues such as the frequency of precession of magnetic moments and the damping mechanism operative in magnetic nanostructures is a topic of interest from the perspective not only of fundamental physics, but from the point of view of contemporary device technology as well. As entities incorporated into devices become smaller and smaller, the physics of spin motions with spatial gradients emerges as a central issue. We see this from the discussions of the injection of spin polarized currents into ultrathin ferromagnets through use of both point contact devices and spatially resolved optical excitation¹. Useful insight into the influence of finite wave vector effects on the frequencies, character of spin wave eigenvectors, and damping may be obtained through the study of finite wave vector spin excitations in ultrathin ferromagnetic films of finite extent.

We have been engaged in theoretical studies of the nature of spin waves in ultrathin ferromagnets, both free standing and adsorbed on metal substrates, along with their damping. These calculations are based on use of an itinerant electron description of the ferromagnetism in the film, and a realistic electronic structure of the the film/substrate combination. Details of our approach may be found in our study of the Fe[110] monolayer on W [110]². We initially concentrated our efforts on the systematic features of these modes, throughout the appropriate two dimensional Brillouin zone^{2,3,4,5}. A focus was placed on the strong intrinsic damping of these modes, which increases dramatically as one moves from the center of the Brillouin zone out to large wave vectors. A striking prediction emerged from these studies. Very near the zone center, the lowest lying acoustical spin wave mode has a very long lifetime, whereas even the first standing spin wave mode suffers substantial damping. For an N layer film, with N in the vicinity of six or eight, the higher frequency standing waves are so heavily damped they are barely perceptible, if at all, in our calculated spectral functions. As one moves out into the Brillouin zone, the damping becomes so severe that one is left only with a single broad feature in the spin fluctuation spectrum, whose peak displays dispersion

expected of a spin wave mode. This picture contrasts dramatically with that provided by a Heisenberg model of a film with localized magnetic moments coupled together by exchange interactions. In such a picture, for each wave vector in the two dimensional Brillouin zone, one has N spin wave modes, and each mode has infinite lifetime. A discussion of the nature of the modes of such a Heisenberg film has been given by one of the authors some decades ago⁶ and we refer the reader to a review article which covers early theoretical studies of spin waves at the surface of Heisenberg magnets, and in films⁷. In regard to ultrathin metallic ferromagnets on metallic substrates, we now have in hand beautiful spin polarized electron loss data which confirm our predictions regarding the nature of the spin wave modes in such systems⁸. We obtain an excellent quantitative account of both the dispersion with wave vector of the single, heavily damped feature found in the experiments, as well as its width and asymmetric lineshape⁵.

The damping mechanism operative in these analyses is, from the point of view of many body physics, a magnetic analogue to the well known Landau damping process responsible for the heavy damping experienced by plasmons in simple metals. One sets up a coherent collective mode of the plasma at time $t = 0$ (the plasmon of metal physics), and the amplitude of the collective mode decays with time as its energy is transferred to incoherent particle hole pairs. Interestingly, for the ideal, collisionless plasma, this transfer does not involve energy dissipation, and is reversible. Thus, one may observe plasma echoes in the presence of Landau damping⁹. In the case of itinerant ferromagnets, the spin wave is a collective oscillation whose nature is very similar to the plasmon in a metal, when viewed in the framework of many body physics¹⁰. This mode may also decay to particle hole pairs, very much as in the plasmon case. In the ferromagnet, conservation of spin angular momentum in the decay process requires the particle hole pairs to be spin triplet excitations. These are commonly referred to as Stoner excitations in the literature on itinerant ferromagnetism⁹. We pause to remark that an intriguing possibility which emerges from this analogy is that of observing FMR echoes which would be the FMR analogue of the plasma echoes just discussed. An ideal sample would be an ultrathin ferromagnet deposited on a non magnetic substrate of finite thickness, with thickness small compared to the spin diffusion length. An example of such a system would be a Ag film grown on GaAs (100), followed by an ultrathin Fe film which is possibly capped with Ag.

When an ultrathin ferromagnet is adsorbed on a metallic substrate, in our studies we

and that the decay process is far more efficient than in a bulk ferromagnet with the same atomic constituents. Hence one finds very short lifetimes for the large wave vector modes. The decay of the collective spin wave to the Stoner excitation spectrum of the $\text{Im}/\text{substrate}$ combination leads to a spin current which transports angular momentum from the ferromagnetic Im into the substrate, hence leading to a decrease in the transverse magnetization associated with the spin motion in the ferromagnet. This same mechanism has been discussed and analyzed in the literature on the ferromagnetic resonance linewidths; in essence one is discussing the lifetime of the acoustic spin wave mode of zero wave vector. In the FMR literature, this is referred to as the spin pumping contribution to the linewidth. Spin pumping was proposed as an important source of FMR linewidths in ultrathin Im s by Berger and Slonczewski, in seminal papers¹¹. These authors employed a simple model description of a Im of localized, Heisenberg like moments coupled to a bath of conduction electrons. Spin pumping was observed experimentally by Woltersdorf and his colleagues¹² and many others since that time. Subsequent theoretical studies provided a very good account of the data¹³. In a recent paper, we have explored the predictions which follow from our approach to spin wave damping. For Fe/Im s grown on a $\text{Au}(100)$ substrate, we obtain an excellent quantitative account of the data in ref. 14. We also obtain a very fine theoretical description of systematics of the linewidth found in trilayers grown on the $\text{Cu}(100)$ surface¹⁵. Thus, our method appears to provide a very satisfactory description of intrinsic linewidths observed in SPEELS studies of large wave vector spin waves in the $\text{Co}/\text{Cu}(100)$ system, and also the linewidth found for the zero wave vector spin wave in FMR studies of Fe on $\text{Au}(100)$.

The present paper presents studies which address the connection between the very small (zero, essentially) wave vector modes studied in FMR and the large wave vector regime addressed in the SPEELS study of the $\text{Co}/\text{Cu}(100)$ system. Two issues are addressed here. First, in regard to the spin pumping contribution to the linewidth, we explore its wave vector dependence. We also examine the nature of the eigenvectors of the low lying spin waves in the Im as one moves away from the zone center into the Brillouin zone. Here we find behavior for the $\text{Fe}/\text{Au}(100)$ system that is very striking. The two lowest lying spin wave modes evolve into waves in which one (the lowest) localizes on the interface between the substrate and the Im as wave vector increases, whereas the second mode localizes on the outer surface of the Im . We argue that a very similar picture applies to the very different $\text{Co}/\text{Cu}(100)$ system as well, though the physics is obscured by the heavier damping found in

the latter system, in the relevant regime of wave vector. If, then, one wishes to interpret the SPEELS data in terms of a simple picture of spin wave modes in the Im , the SPEELS loss spectrum would receive its dominant contribution not from the lowest lying mode in the Im , as proposed by the authors of ref. 8, but rather the second mode in the hierarchy of spin wave modes of the Im . We note that we set forth this proposal in our earlier publication⁵, and the results presented in this paper reinforce this interpretation. The comparison we make between these two ultrathin Im s of different crystal structure suggests in our mind that the behavior we find may be expected rather generally in the ultrathin ferromagnets.

The outline of this paper is as follows. In section II we provide the reader with a brief summary of the early theoretical analyses of the nature of low lying spin wave modes in Heisenberg Im s. These studies, very relevant to our present discussion, are not so well known in the present era so a reminder of the concepts which follow from these papers will provide a setting for what emerges from the work reported here. We then present our results in section III, and concluding remarks are found in section IV.

II. SURFACE SPIN WAVES ON HEISENBERG FERROMAGNETS

We begin by considering an ideal semi infinite Heisenberg ferromagnet. The term ideal here describes a model system in which the strength of the underlying exchange interactions in and near the surface assume the same values as they do in the bulk material. In such a case, one may envision forming two semi infinite crystals by beginning with an infinitely extended crystal, and then cutting all exchange bonds which cross a mathematical plane between two atomic planes.

Through study of one particular model surface, Wallis and co workers¹⁶ pointed out that such an ideal surface can support surface spin waves, with amplitude that decays exponentially as one moves into the crystal from the surface. The properties of the surface wave found by these authors differ strikingly from those of the more familiar Rayleigh surface phonons which propagate on crystal surfaces. In the bulk of the material, and in the long wavelength limit we know well that the frequency of spin waves varies quadratically with wave vector. We have $\hbar\omega(\vec{Q}) = DQ^2$ in cubic crystals. The surface spin wave studied in ref. 16 exists for all wave vectors in the surface Brillouin zone. If one considers the surface spin wave with two dimensional wave vector \vec{Q}_\parallel , its frequency lies below that of the manifold

of bulk spin waves whose wave vector projection onto the plane of the surface assumes the value Q_{\parallel} . However, in the long wavelength limit the frequency of the surface spin wave is $\hbar\omega_s(Q_{\parallel}) = D Q_{\parallel}^2$, with D the bulk exchange stiffness. The binding energy of the surface spin wave in the long wavelength limit arises from the terms quartic in the wave vector. In contrast, in the long wavelength limit, the Rayleigh surface phonon propagates with velocity less than that of any bulk phonon with the same wave vector parallel to the surface, so the surface wave and bulk wave dispersion curves differ to leading order in Q_{\parallel} . As noted earlier, the amplitude of the surface spin wave discussed in ref. 16 decays to zero exponentially as one penetrates into the bulk material. If one describes this by the expression $\exp[-(Q_{\parallel})l_z]$ where l_z labels an atomic plane, one finds (Q_{\parallel}) is proportional to Q_{\parallel}^2 in the long wavelength limit, whereas for the Rayleigh surface phonon, the decay constant is linear in Q_{\parallel} . While the authors of ref. 16 studied one specific model of an ideal Heisenberg ferromagnet surface, subsequent discussions showed that the features just discussed are robust and follow for a very wide range of models of the surface, including those in which exchange interactions near the surface differ substantially from those in the bulk^{6,7}. For the ideal surface, the criterion for the existence of surface spin waves is as follows⁶. When the surface is formed by the bond cutting procedure described earlier, one must cut exchange bonds which are non-normal to the surface.

While we are not concerned in the present paper with the nature of thermal spin fluctuations at finite temperature in our model, interesting issues arise when one discusses the near surface behavior of thermal spin fluctuations. The surface spin waves are eigenmodes of the Heisenberg Hamiltonian and thus are present as thermally excited spin waves. However, if one calculates the amplitude of thermal fluctuations in the magnetization near the surface, in the low temperature limit the contribution from the surface spin waves is exactly and precisely cancelled by a deficit in the density of bulk spin waves which results from the formation of the surface wave; there is a hole in the density of bulk spin wave modes that leads to this cancellation. This was demonstrated first for the model studied in ref. 16, and later shown to be robust^{6,17} and insensitive to the microscopic details of the surface environment. In the end, one finds that the amplitude of the thermal fluctuations in the surface is twice that deep in the bulk of the material, and one may derive an analytic expression for the dependence of the mean spin deviation as a function of distance into the material from the surface^{6,17}, in the limit of low temperatures.

We now turn our attention to Im s. If we have an isolated Im with two identical surfaces, then of course all the spin wave eigenvectors must have well defined parity under reflection through the midpoint of the Im . Suppose we consider a wave vector Q_{\parallel} in the surface Brillouin zone sufficiently large that the quantity $(Q_{\parallel})^2$ introduced above satisfies $(Q_{\parallel})^2 N > 1$, with N the number of atomic layers within the Im . Then the two lowest lying modes of the Im with wave vector Q_{\parallel} will have the character of surface spin waves. One mode (that with the highest frequency, for reasons to be given below) will be odd under reflection through the Im with a displacement pattern that decays exponentially as one moves into the interior of the Im from either surface, and the other will be even parity also with displacements localized near the surfaces. The frequency splitting between the two modes will be proportional to $\exp[-2(Q_{\parallel})^2]$.

Now suppose, for the Im just discussed, we let $Q_{\parallel} \rightarrow 0$. As we proceed with this limit, we enter the regime where $(Q_{\parallel})^2 N < 1$, and the two surface mode eigenvectors must continuously and smoothly evolve into the two lowest lying $Q_{\parallel} = 0$ modes of the finite Im . The lowest of these has zero frequency (in the absence of an applied Zeeman field), and is the uniform mode of the Im , wherein all spins precess rigidly and in phase. This is an even parity mode. The next highest mode is an odd parity standing wave mode whose eigenvector vanishes at the midpoint of the Im . The perpendicular wave vector assumes the value π/N as $Q_{\parallel} \rightarrow 0$, so this mode has finite, non zero frequency. The odd parity mode thus has higher frequency than the even parity mode, and one thus expects the odd parity mode to have the higher frequency throughout the surface Brillouin zone, though of course in principle one may have Im parameters in which a crossing of the dispersion curves occurs.

These comments provide us with a setting for the results we shall present below which, of course, are based on a fully itinerant electron description of the spin waves in our Im . One important difference between the Im we consider here, and the Heisenberg Im with two identical surfaces is that in our case the two surfaces are inequivalent. One is the interface between the Im and the substrate upon which it is absorbed, and the second is the outer surface, with vacuum above. We shall see that at the center of the Brillouin zone, we find the lowest mode to be the uniform mode, whose eigenvector is modified however, by the enhanced moment at the Im vacuum interface. The next highest mode looks very much like the first odd parity standing wave. As the wave vector increases, rather than

realize the even and odd parity surface waves, we shall see that the lower mode localizes near the $\text{Mn}/\text{substrate}$ interface, whereas the second mode (not strictly odd parity for our Mn), localizes on the outer surface. In our earlier study⁵ of the Co/Mn on $\text{Cu}(100)$, we used adiabatic theory to calculate effective Heisenberg exchange interactions between various nearest and next nearest neighbor moments. As one sees from Table II, at the outer surface, and in the layer against the substrate the nearest neighbor exchange interactions are enhanced substantially over the values deep in the Mn , with the effective exchange on the outer surface larger than that at the interface between the substrate. Such enhanced effective exchange plays an important role in binding the spin waves to the surface, and to the $\text{Mn}/\text{substrate}$ interface.

III. PROPERTIES OF INTERMEDIATE WAVE VECTOR SPIN WAVES FOR $\text{Fe}/\text{Au}(100)$ AND FOR $\text{Co}/\text{Cu}(100)$

As remarked above, we have used the programs developed for our analysis of the spin pumping linewidth for the Fe/Mn on $\text{Au}(100)$ to explore the nature of the spin waves in the Fe/Mn and their damping near the center of the Brillouin zone. We begin by presenting these results, and then we turn to our considerations for the Co/Mn on $\text{Cu}(100)$. The first mentioned system was used in the experimental studies of the spin pumping contribution to the FMR linewidth by Urban and collaborators¹², and large wave vector spin waves in the second system were explored in the SPEELS experiments reported by Vollmer and coworkers⁸.

The results below were extracted from studies of the wave vector and frequency dependent susceptibility $\chi_{\pm}(\mathcal{Q}; \mathbf{l}_1; l^0)$ of four and eight layer $\text{Fe}(100)$ Mn s adsorbed on the $\text{Au}(100)$ surface. From this response function, we form the spectral density function $A(\mathcal{Q}; \mathbf{l}_1; \mathbf{l}_2) = \frac{1}{2} [\chi_{\pm}(\mathcal{Q}; \mathbf{l}_1; l^0) + \chi_{\pm}(\mathcal{Q}; \mathbf{l}_2; l^0)]$. From the spectral density function we may extract the dispersion relation of the spin wave modes by following the trajectory with wave vector of the resonant peaks in this response function, and the linewidth is obtained from the width of these structures. Information on the nature of the eigenvectors may be obtained from the transverse susceptibility itself through a procedure described below. We refer the reader to section II of ref. 14 for a discussion of the physical significance of these two quantities.

When we plot the dispersion curves of the two lowest lying spin wave modes for the Fe/Mn

near the center of the Brillouin zone, we find a most interesting level crossing, as illustrated in Fig. 1. In Fig. 1(a), we show the dispersion relation of these two modes for the four layer Fe(100) film on Au(100), for wave vectors along the $[11]$ direction. With increasing wave vector, the lowest lying mode shows positive curvature, while the first standing wave mode shows negative curvature. The two dispersion curves start to cross, and we see a hybridization gap. We note that the hybridization gap is a feature present by virtue of the fact that the two surfaces of the film are distinctly different; at the outer surface of the film, we have an interface with the vacuum, and the inner surface is the interface with the substrate. In a free standing film, the low frequency mode would have even parity, the first standing wave would have odd parity, and symmetry would then prohibit the mixing that leads to the hybridization gap. We remark that, as in our earlier studies of the spin pumping contribution to the linewidth, we have added a Zeeman field to our Hamiltonian which renders the frequency of the lowest frequency mode finite in the limit of zero wave vector. The field we use is unphysically large, but as discussed earlier¹⁴ so long as the spin wave frequencies are small compared to the energy scale of the one electron band structure, all the field does is to shift all modes upward in frequency by the Zeeman energy. There are computational advantages to introducing this shift. Linewidths are linear in frequency at zero wave vector, as we have shown earlier¹⁴ so when we plot the ratio of the linewidth to the frequency of the mode, we have a ratio independent of applied field so long as the spin wave frequencies are low. In Fig. 1(b) we show dispersion curves for the eight layer film. We see, as expected, the exchange contribution to the frequency of the first standing wave mode is quite accurately four times less than that found for the four layer film.

In Fig. 2, for the eight layer film we plot the spectral density function $A(Q_{\parallel}; l_2)$ as a function of frequency, for various layers in the film. The layer labeled I at the top of each plot is the interface between the film and the substrate, while the lowest layer labeled S is the outer surface layer. The leftmost panel shows the spectral densities for zero wave vector, whereas the rightmost panel gives these for a reduced wave vector of 0.25. As explained earlier,¹⁴ the integrated intensity of each peak can be interpreted as the square of the eigenvector of the mode associated with the peak. In the leftmost panel, we see that the low frequency mode is indeed the uniform mode of the film. It is the case that the amplitude in the surface is somewhat larger than in the inner layers. This is an effect with origin in the enhanced surface moment at the surface/vacuum interface. The higher frequency mode

is clearly a classical standing wave, with an eigenvector when squared has a cosine squared variation layer number, and a node in the center of the In . The wavelength perpendicular to the In is twice the In thickness.

As wave vector increases, we see from the rightmost panel in Fig. 2, the lower mode becomes a localized spin wave mode, with eigenvector localized at the In /substrate interface. The high frequency mode evolves into a surface spin wave, localized on the outer surface. Interestingly, the higher frequency mode is narrower than the low frequency mode. Our previous studies suggest that the broadening at fixed wave vector parallel to the surface increases with the gradient in the eigenvector in the direction normal to the surface. The low frequency mode is considerably more localized than its higher frequency partner, which suggests it should indeed be broader.

In Fig. 3, we in (a) we show the wave vector dependence of the linewidth divided by the mode frequency for the four layer In , and in (b) we show this for the eight layer In . At zero wave vector, we have the spin pumping contribution to the linewidth we¹⁴ and others^{11,13} have discussed earlier. This falls off inversely with the thickness of the ferromagnetic In . The solid line in these figures assumes that the wave vector dependent portion of the linewidth scales as Q^4 , and we see this fits the data very well indeed over a rather wide range of wave vectors near the center of the Brillouin zone.

A simple argument shows that the linewidth must vary as the fourth power of the wave vector, as we find numerically. We illustrate this for a very simple case, spin waves in an infinitely extended ferromagnet as described by the random phase approximation applied to the one band Hubbard model. It is our view that this conclusion applied to our much more complex system as well, but the formal analysis will be very involved. We remark that the argument presented below is applicable to multi band descriptions of the spin waves in the bulk, if the Lowde Windsor parametrization¹⁸ of the on site Coulomb interaction is employed.

For this simple case, the dynamic susceptibility has the well known form

$$\chi_{+;}^{(0)}(Q; \omega) = \frac{\chi_{+;}^{(0)}(Q; \omega)}{1 + U \chi_{+;}^{(0)}(Q; \omega)} : \quad (1)$$

If we write $\chi_{+;}^{(0)}(Q; \omega) = \chi_{+;}^{(0)R}(Q; \omega) + i \chi_{+;}^{(0)I}(Q; \omega)$, then the spectral density function

which contains the spin wave signature is

$$A(Q; \omega) = \frac{1}{\hbar} \frac{\chi_{+;+}^{(0)I}(Q; \omega)}{1 + U_{+;+}^{(0)R}(Q; \omega) + U_{+;-}^{(0)I}(Q; \omega)} \quad (2)$$

In the long wavelength limit, the quantity $1 + U_{+;+}^{(0)R}(Q; \omega)$ has a zero at the spin wave frequency $\omega(Q) = DQ^2$. We then expand $\chi_{+;+}^{(0)R}(Q; \omega)$ as follows:

$$\chi_{+;+}^{(0)R}(Q; \omega) = \chi_{+;+}^{(0)R}(Q; \omega(Q)) + \chi_{-+}^{(0)R}(Q; \omega(Q)) \frac{\hbar}{\omega(Q)} + \dots \quad (3)$$

The imaginary part of $\chi_{+;+}^{(0)}(Q; \omega)$ vanishes at zero frequency, and this function is linear in frequency for small frequencies. Hence in the limit of small wave vector, we may write $\chi_{+;+}^{(0)I}(Q; \omega(Q)) = \chi_{+;+}^{(0)I}(Q; DQ^2) = DQ^2 \chi_{-+}^{(0)I}(Q; 0)$. It is simple to show from the explicit expression for $\chi_{+;+}^{(0)}(Q; \omega)$ that $\chi_{-+}^{(0)I}(0; 0)$ vanishes, and also that $\chi_{-+}^{(0)I}(Q; 0)$ is an even function of wave vector. Hence, for small values of the wave vector one may write $\chi_{-+}^{(0)} \approx bQ^2$ so that we have $\chi_{+;+}^{(0)I}(Q; \omega(Q)) \approx bDQ^4$. We may then, in the low frequency long wavelength limit make the replacement $\chi_{-+}^{(0)R}(Q; \omega(Q)) \approx \chi_{-+}^{(0)}(0; 0)$ in Eq. 3. The spin wave density can then be written, in the long wavelength low frequency limit as

$$A(Q; \omega) = \frac{m}{\hbar} \frac{Q^4}{[DQ^2]^2 + [Q^4]^2} \quad (4)$$

Here $m = n_{\#} \chi_{+;+}^{(0)R} = mU^2bD$, and we have used $\chi_{-+}^{(0)R} = 1 = U^2m$.

It follows from Eq. 4 that for the models of bulk spin waves encompassed by the above discussion the linewidth scales as the fourth power of Q very much as we find for our numerical studies in the ultrathin films. In the film calculations, we obtain a finite linewidth at zero wave vector by virtue of the applied Zeeman field. Even if a Zeeman field is applied to the bulk, at zero wave vector the linewidth of the uniform mode must vanish by virtue of the Goldstone theorem applied to the Hamiltonian, which is form invariant under spin rotations. As we have argued earlier¹⁴, in the ultrathin films, the breakdown of translational symmetry normal to the surface allows a finite linewidth when the wave vector parallel to the surface is zero; the mode is not a uniform spin precession in the entire system of the film-substrate combination.

The spectral density plots shown in Fig. 2 provide information on the variation of the square of the eigenvector of a particular mode, as one scans through the layer number in the film. We have devised a means for extracting the eigenvector itself from the function

$+, (\omega = \omega_j; \mathbf{l}_1; \mathbf{l}_2^0)$. We first evaluate, for a selected value of $\omega = \omega_j$, the response function at the frequency $\omega = \omega_j$ of the mode of interest. This frequency is chosen to be the frequency of a selected peak in a spectral density plot such as those in Fig. 2. Then the eigenvector is generated from the eigenvalue problem

$$\sum_{\mathbf{l}_2^0} X_{+, (\omega = \omega_j; \mathbf{l}_1; \mathbf{l}_2^0)} e^{i(\omega = \omega_j) \mathbf{l}_2^0} = (\omega = \omega_j) e^{i(\omega = \omega_j) \mathbf{l}_1} : \quad (5)$$

The eigenvectors generated by this scheme are in general complex, with an amplitude and a phase.

In Fig. 4, we show the amplitude and phase of the eigenvector associated with the lowest mode in the eight layer Fe film on Au. The top two panels show the modulus and phase of the eigenvector at the center of the two dimensional Brillouin zone. We see the mode is indeed nearly uniform across the film. The increased amplitude in the surface layer has its origin in the fact that in the outer layer, the moment is larger than it is in the middle of the film. Notice the phase is zero across the film, so the various layers precess in phase, as expected from simple phenomenology. The lower two panels show the amplitude and phase of the mode at the reduced wave vector of 0.25 in the [11] direction. The leftmost layer labeled I is the interface with the substrate, and the rightmost layer is the outer surface layer. We see the mode is quite localized near the interface.

We show the same information for the second mode of the film in Fig. 5. At the center of the Brillouin zone, the amplitude and phase information show a mode whose profile is rather closely described by the simple standing wave pattern $\cos[(\mathbf{l}_2 - \mathbf{l}_1) = \pi]$ expected for the lowest standing wave mode in the film, with one half wavelength trapped between the surfaces. The profile is distorted a bit from this form by the enhancement of the amplitude in the outer surface layer, as in the uniform mode. By the time the reduced wave vector is 0.25 (two lower panels), we see that the mode is localized on the outer surface.

We next inquire if similar behavior is found for the Co film on Cu(100) which we have studied earlier. When we explore this issue within the full dynamical theory used above, we see very similar trends. However, the hybridization between the two lowest spin wave modes and also their tendency to localize at the interface with the substrate or the surface appears to occur somewhat farther out in the Brillouin zone. In this region, the damping has become sufficiently severe that we have not been able to extract clear eigenvectors for the two modes utilizing the method we have employed for the case of Fe on Au(100). To examine this

question for this system, we have resorted to calculations based on the Heisenberg model for this film. In our previous publication, in Table II we provide values for the exchange interactions between all nearest and next nearest neighbors, for the eight layer Co film on Cu(100). Interestingly, we see strong enhancement of the exchange interactions between nearest neighbors in both the surface layer, and also those within the layer closest to the interface.

In Fig. 6, the left hand figure shows the eigenvector of the lowest mode at zero wave vector (open circles), and at a reduced wave vector of 0.6 (triangles). In the Heisenberg model, the eigenvectors are real, it should be remarked. We see that once again the lowest mode becomes localized onto the interface layer with increasing wave vector. The right hand panel shows the second mode at the center of the Brillouin zone (open circles) and its behavior at the reduced wave vector of 0.6 (triangles). We see behavior very similar to that found for Fe on Au(100). It is also the case here, for instance, that the lowest mode is localized more strongly to the interface than the second mode is to the surface. In Fig. 7, we show the dispersion curve calculated for these two modes, along the $[11]$ direction in the zone. Despite the very different character of their eigenvectors, the splitting in frequency of the two modes is rather small throughout the zone. Thus, except near the zone center it is difficult for us to resolve these two modes in the full dynamical calculations.

IV. CONCLUDING REMARKS

We have presented studies of the nature of the spin wave modes, and the wave vector dependence of their damping for the two low lying modes of Fe films on the Au(100) surface. The mode excited in FM R, the uniform mode at the center of the two dimensional Brillouin zone, evolves into the mode localized at the interface between the film and the substrate with increasing wave vector. The next highest mode in frequency, a standing wave spin wave at the center of the Brillouin zone, evolves into a surface spin wave with increasing wave vector. We remark that while there is an extensive literature on the nature of surface spin waves in Heisenberg magnets⁷, we are unaware of any other study of surface or interface spin waves within the framework of a discussion that employs a realistic electronic structure and an itinerant electron description of the ferromagnet. We do wish to point out Mathons very interesting studies of surface spin waves on the (100) surface of a one band Hubbard

model¹⁹. In his first paper, he makes explicit contact with properties of surface spin waves generated from Heisenberg models, and in the second paper a discussion is given in terms of adiabatically calculated exchange integrals, generated from the itinerant electron picture. To return to the results presented here, we see also that with increasing wave vector, the wave vector dependent contribution to the damping rate of the lowest mode in the In increases as Q^4 . We find very similar behavior for the two lowest lying spin wave modes for the eight layer Co on $\text{Cu}(100)$, though since the localization phenomenon takes place farther out in the Brillouin zone, we have had to resort to a Heisenberg model description of these waves. These two examples for In s with a very different structure suggests to us that this behavior may be expected for other systems as well.

There are two implications of the results discussed above. First, in the SPEELS study of the spin waves for Co on $\text{Cu}(100)$, Vollmer et al. suggested that their spectra received its dominant contribution from the lowest lying spin wave mode of the In . The results here suggest this is not so, since the lowest mode appears to localize at the In /substrate interface with increasing wave vector, with the consequence that its amplitude in the surface layer sampled by the SPEELS electrons is in fact very small. It is the second mode which appears to localize on the outer surface. Thus, if one wishes to interpret the spectra in terms of a single mode, the lowest lying mode of the In is not the correct choice. Of course, have emphasized earlier^{2,3,4,5}, except rather near to the zone center, the damping of the spin wave modes in these ultrathin In s is sufficiently strong that it is difficult to assign the single very broad structure found in the spectral density to a selected mode.

A second implication follows from the wave vector dependence we find for the linewidth. In ref. 1, where finite wavelength spin waves were excited in an ultrathin ferromagnet, it was argued that the data indicates the damping to be strongly wave vector dependent. These authors argued that two magnon scattering^{20,21} was responsible for the wave vector dependence inferred from this data. The In s in ref. 1 were grown on exchange biased substrates. We note that in earlier work, direct measurements of the wave vector dependence of the spin wave linewidth in such samples were reported and found to be in remarkable agreement with the theory of two magnon damping²². We show here that there is also a strong wave vector dependence to the spin pumping contribution to the linewidth of long wavelength spin wave modes in the itinerant ferromagnetic In s. However, because of the Q^4 variation we have found, the effect is small until one reaches wave vectors in the range of

10^7 cm^{-1} . Thus, for the purposes of the data in ref. 1, which explore much longer wavelength modes, one can regard the spin pumping contribution to the wave vector dependence of the damping rate to be quite negligible. Our results thus reinforce the interpretation offered in ref. 1.

Acknowledgments

The research of D.L.M. was supported by the U.S. Department of Energy, through grant no. DE-FG 03-84ER-45083. A.T.C. and R.B.M. have received support for the CNPq, Brazil. A.T.C. also acknowledges the use of computational facilities of the Laboratory for Scientific Computation, UFPA, Brazil.

-
- ¹ For an example of point contact excitation of spin waves in spin valves, see W.H. Rippard, M.R. Puffall, S. Kaka, S.E. Russek and T.J. Silva, *Phys. Rev. Letters* 92, 027201 (2004), and excitation of spin waves by focused laser beams has been reported by G.W. Olbersdorf, M. Buess, B. Heinrich, and C.H. Back, *Phys. Rev. Letters* 95, 037401 (2005).
 - ² R.B.M. uniz and D.L.M. ills, *Phys. Rev. B* 66, 174417 (2002).
 - ³ A.T.C. Costa, R.B.M. uniz and D.L.M. ills, *Phys. Rev. B* 68, 224435 (2003)
 - ⁴ R.B.M. uniz, A.T.C. Costa and D.L.M. ills, *Journal of Physics (Condensed Matter)* 15, S495 (2003).
 - ⁵ A.T.C. Costa, R.B.M. uniz and D.L.M. ills, *Phys. Rev. B* 70, 054406 (2004).
 - ⁶ D.L.M. ills, *Phys. Rev. B* 1, 264 (1970).
 - ⁷ D.L.M. ills, Chapter 3 of *Surface Excitations*, edited by V.M. Agranovich and R. Loudon, (North Holland Publishing Company, Amsterdam, 1984).
 - ⁸ R. Vollmer, M. Eitzkom, P.S. Anilkumar, H. Ibach and J. Kirschner, *Phys. Rev. Letters* 91, 147201 (2003).
 - ⁹ R.W. Gould, T.M. O'Neil and J.H. Malinberg, *Phys. Rev. Letters* 19, 219 (1967).
 - ¹⁰ See, for instance, the structure of the magnon wave function described by C. Herring, page 368 of *Magnetism, Vol. IV*, edited by G. Rado and H. Suhl, (Academic Press, N.Y. 1966).

- ¹¹ L. Berger, *Phys. Rev. B* 54, 9353 (1996); J. Slonczewski, *J. Magn. Mater.* 195, L261 (1999).
- ¹² R. Urban, G. Woltersdorf, and B. Heinrich, *Phys. Rev. Letters* 87, 217204 (2001).
- ¹³ Y. Tserkovnyak, A. Brataas, and G. E. W. Bauer, *Phys. Rev. Letters* 88, 117601 (2002); *Phys. Rev. B* 66, 224403 (2002), M. Zwierzycki, Y. Tserkovnyak, P. J. Kelly, A. Brataas, and G. E. W. Bauer, *Phys. Rev. B* 71, 064420 (2005).
- ¹⁴ A. T. Costa, R. B. Muniz and D. L. Mills, *Phys. Rev. B* 73, 54426 (2006).
- ¹⁵ K. Lenz, T. Tolinski, J. Lindner, E. Kosubek, and K. Baberschke, *Phys. Rev. B* 69, 144422 (2004).
- ¹⁶ R. F. Wallis, A. A. Maradudin, I. P. Ipatova, and A. A. K lochikin, *Solid State Communications* 5, 89 (1967).
- ¹⁷ A. A. Maradudin and D. L. Mills, *J. Chem. Phys. Solids* 28, 1855 (1967).
- ¹⁸ R. Lowde and C. G. Windsor, *Adv. Phys.* 19, 803 (1970).
- ¹⁹ J. Mathon, *Phys. Rev. B* 24, 6588 (1981); *Phys. Rev. B* 34, 1775 (1986).
- ²⁰ R. Arias and D. L. Mills, *Phys. Rev. B* 60, 7395 (1999).
- ²¹ D. L. Mills and S. M. Rezende, page 27 of *Spin Dynamics in Connected Magnetic Structures II*, (Springer Verlag, Heidelberg, 2003).
- ²² S. M. Rezende, A. Azevedo, M. A. Lucena, and F. M. de Aguiar, *Phys. Rev. B* 63, 214418 (2001).

Figures

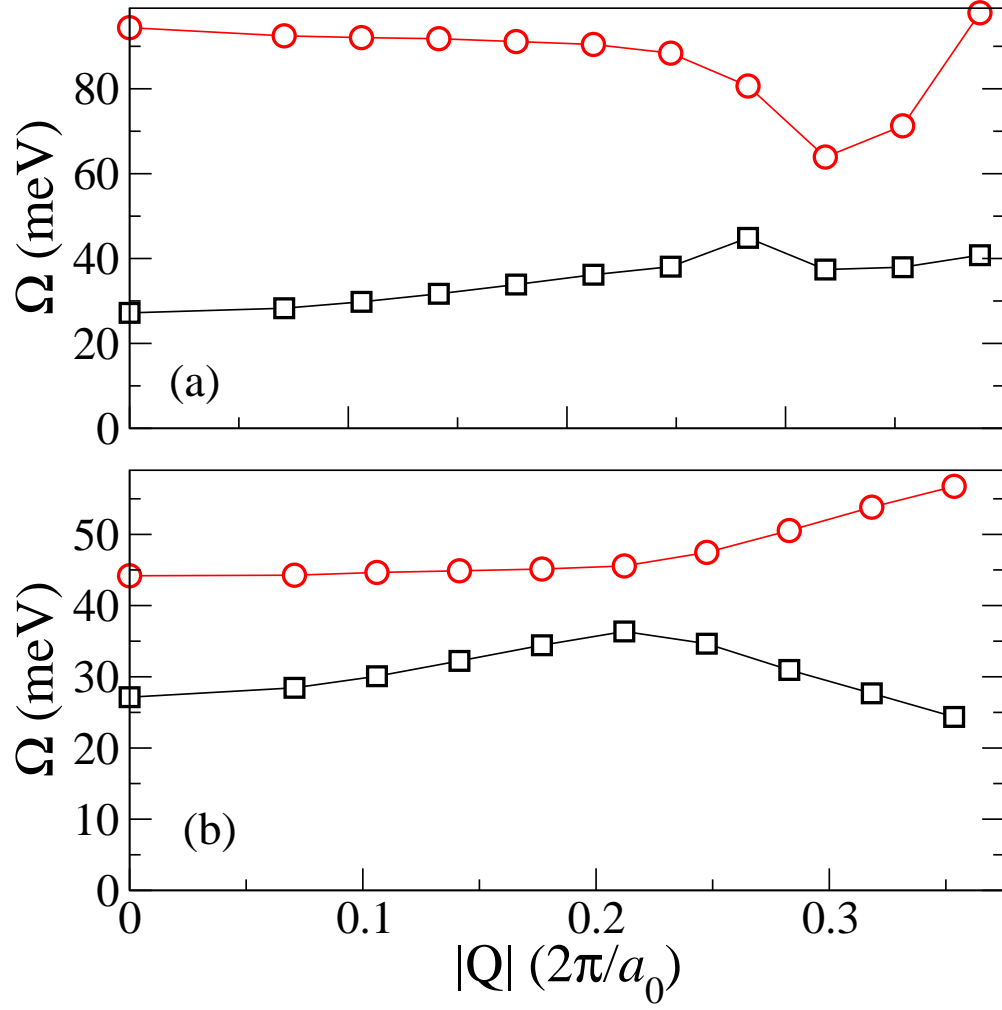


FIG . 1: For the (a) four layer, and (b) the eight layer Fe Mn on Au (100), we show the dispersion relation of the two lowest lying modes of the Mn as a function of reduced wave vector, along the $[11]$ direction in the Brillouin zone. As discussed in the text, a Zeeman field has been imposed so the lowest mode has finite frequency at the zone center.

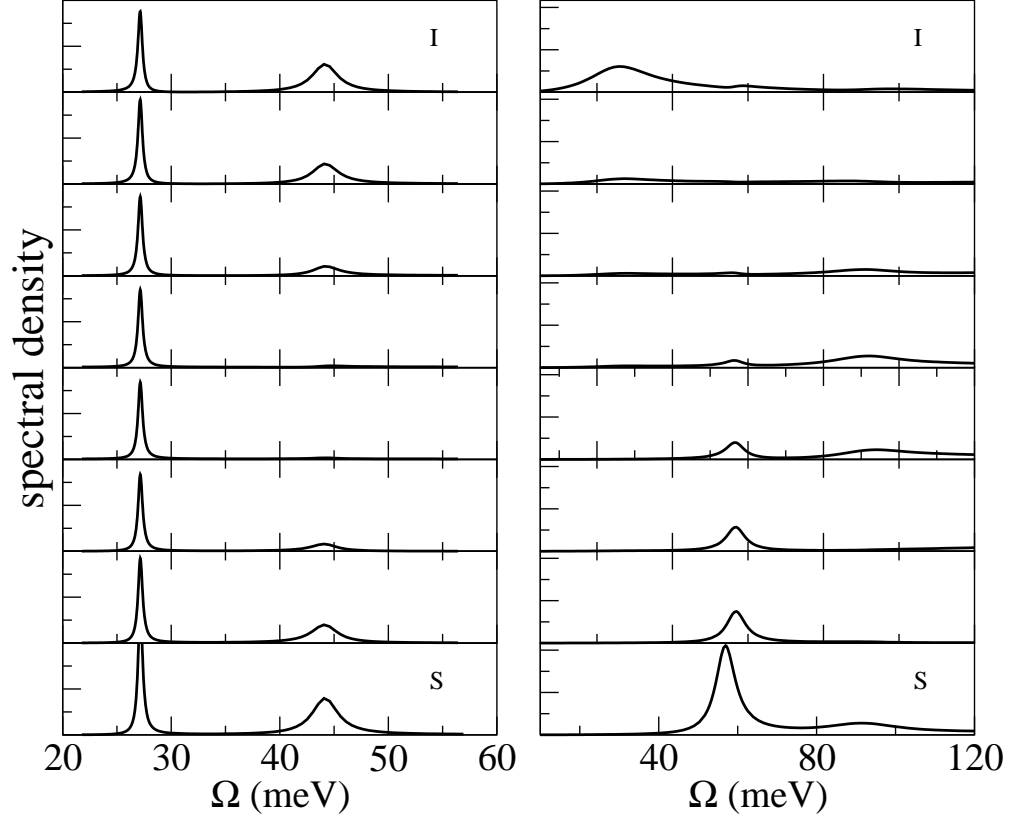


FIG. 2: We plot the frequency variation of the spectral density $A(Q_{\parallel}; \omega; l_z)$ as a function of layer index l_z , for the eight layer Fe/Mn on Au(100) and for two selected wave vectors. In the left panel, we have zero wave vector, and in the right panel the reduced wave vector is 0.25 along the [11] direction. The top entries, labeled I, is the layer adjacent to the Au substrate, and the lowest entry labeled S is the outer surface layer of the Mn.

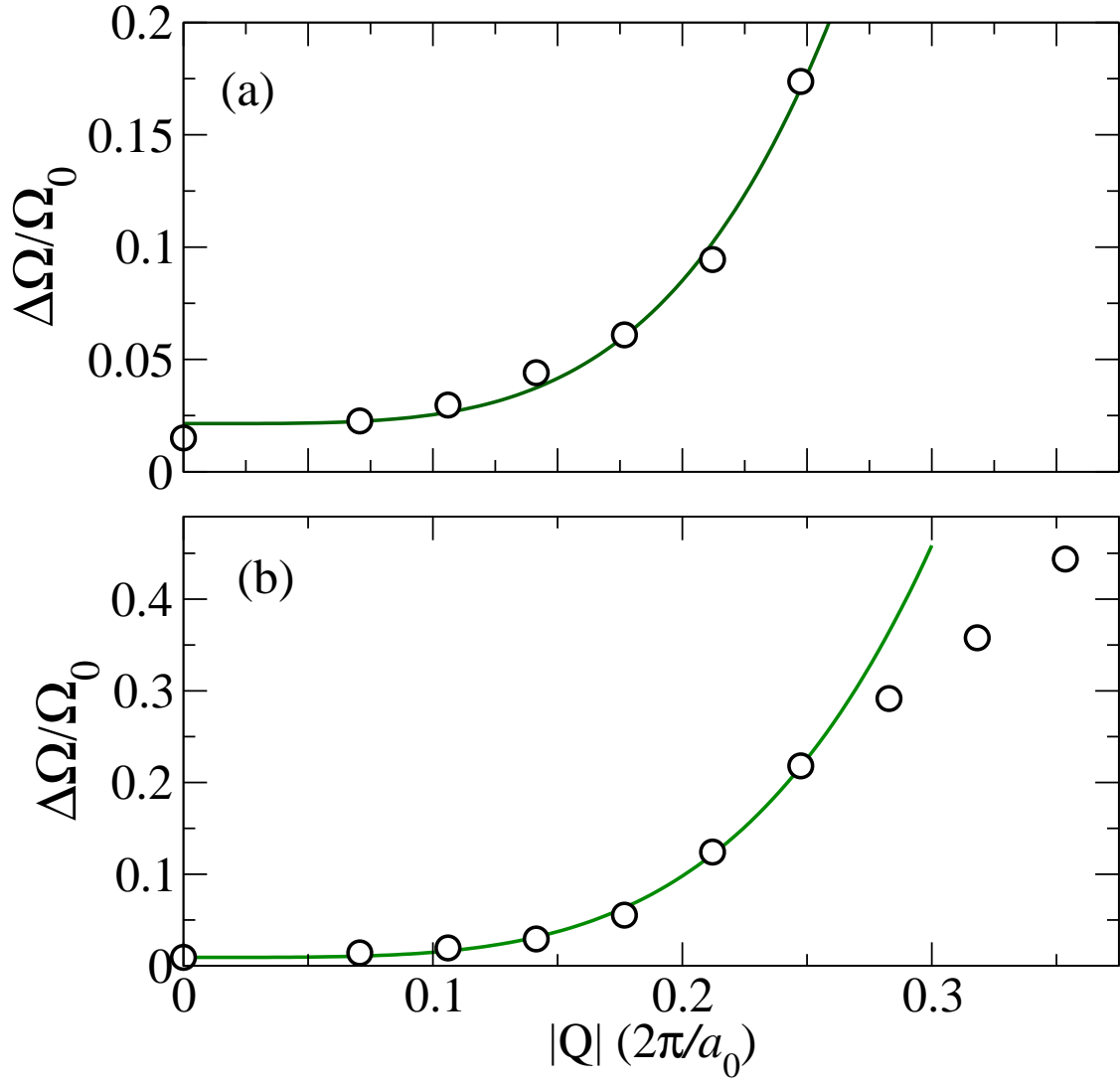


FIG . 3: Linewidths of the lowest mode as a function of wavevector along the $[11]$ direction in a 4 layer (a) and a 8 layer (b) Fe /In on Au (100). The solid curves are fittings to Q^4 functions.

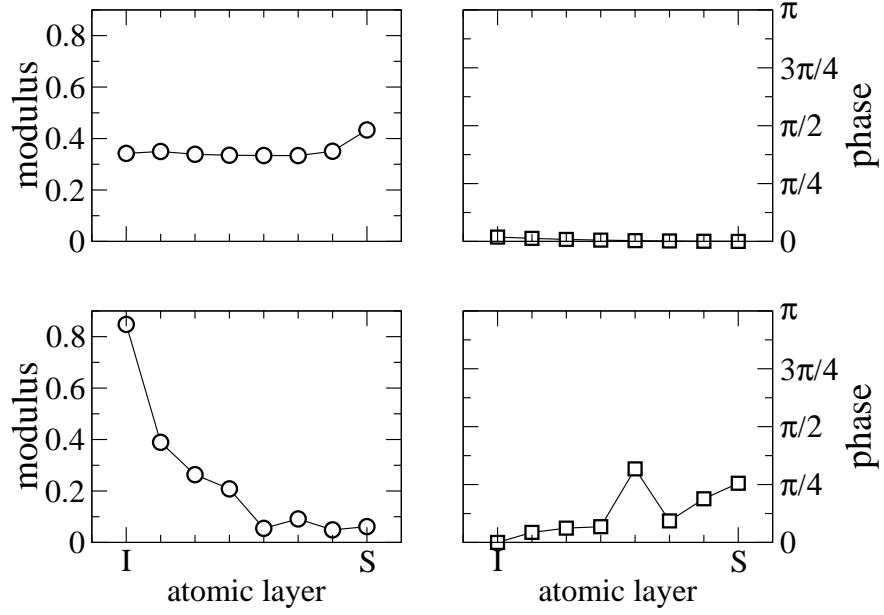


FIG . 4: The amplitude and phase of the eigenvector associated with the lowest frequency mode of the eight layer Fe In on Au(100). The top two panels show the eigenvector of the mode at $Q_{||} = 0$, and the bottom two panels give the same for a reduced wave vector of 0.25 along the $[11]$ direction in the two dimensional Brillouin zone. The layer labeled I is the Fe layer against the substrate, and the layer labeled S is the outermost surface layer of the In .

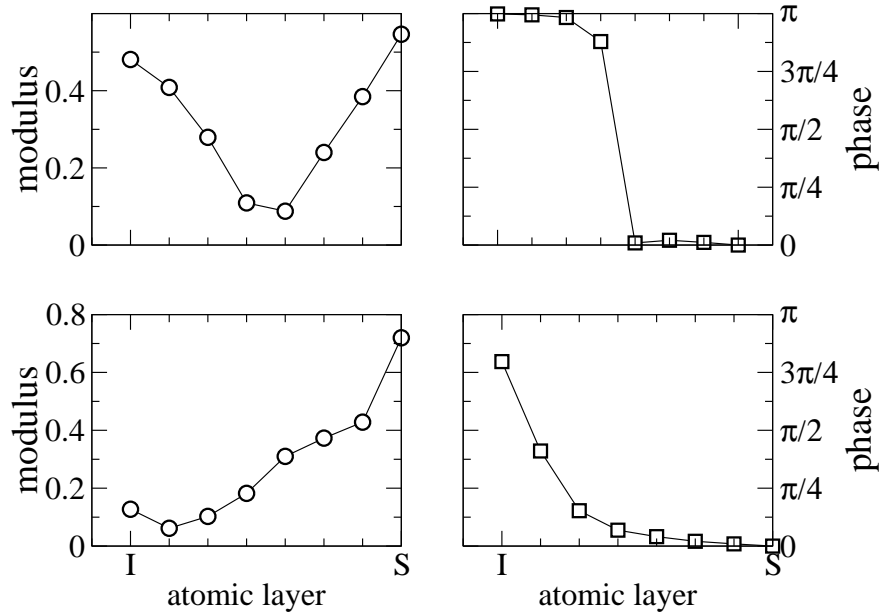


FIG . 5: The same as Fig. 4, but now for the second mode of the In .

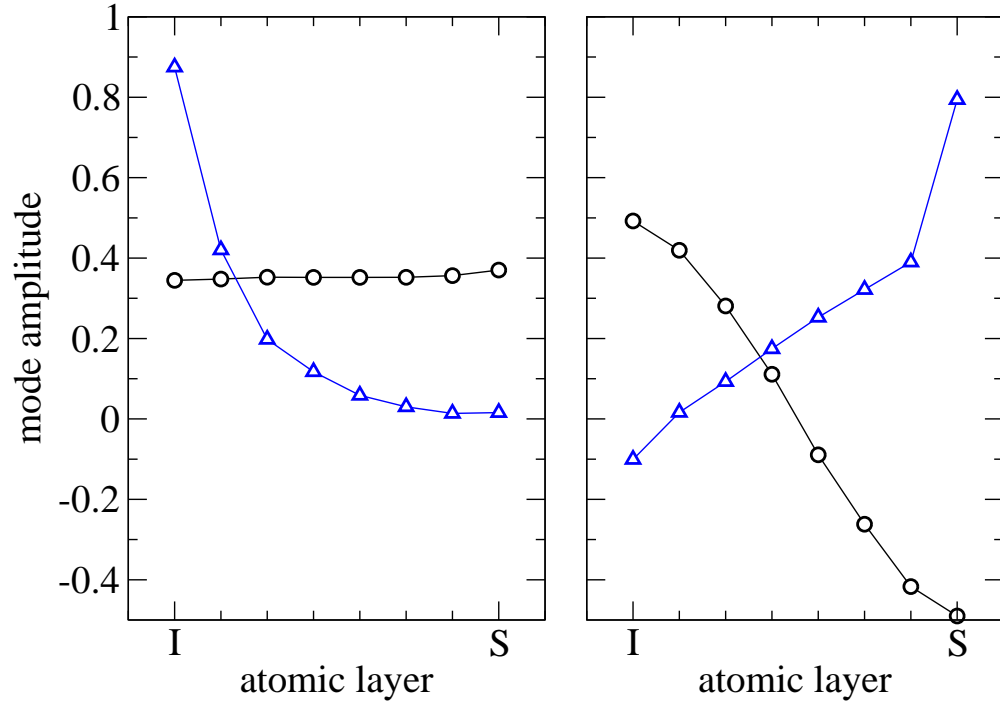


FIG. 6: We show eigenvectors for Co on Cu(100) calculated using the Heisenberg model, as described in the text. The left panel shows the behavior of the lowest mode at the center of the Brillouin zone (open circles), and at the reduced wave vector of 0.6 along the [11] direction in the Brillouin zone. (triangles). The right panel gives the same information for the second mode. The layer labeled I is the layer of Co spins adjacent to the Cu(100) substrate, and the layer labeled S is the outer surface layer.

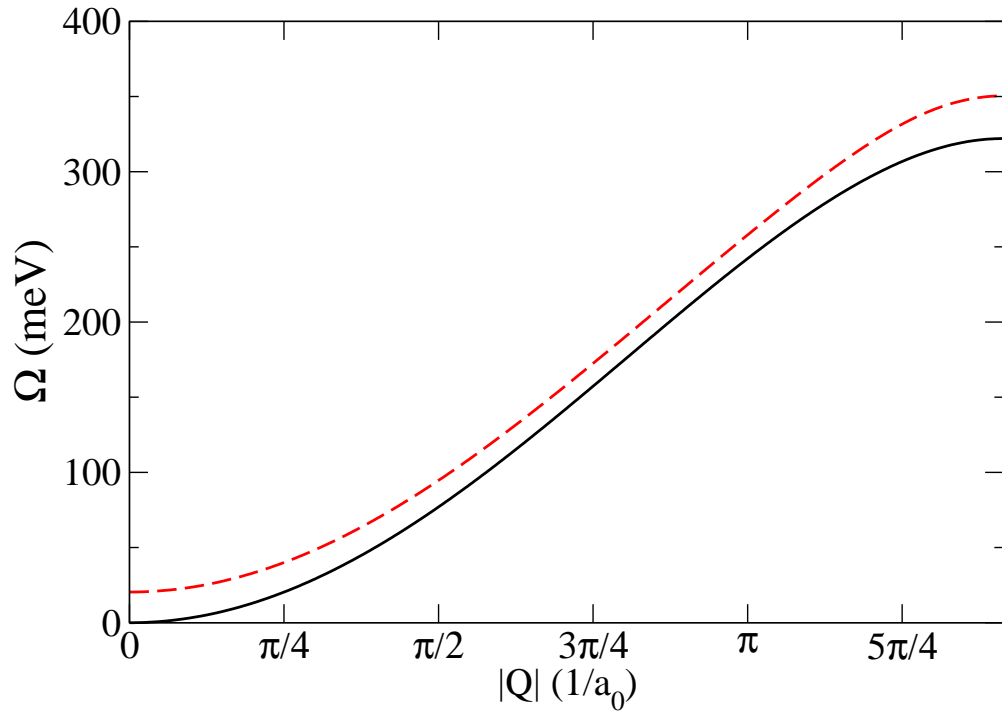


FIG . 7: The dispersion relation of the two lowest lying modes in the Co film on Cu(100). The wave vector is directed along the [11] direction in the two dimensional Brillouin zone.